Introduction

Black dots of amorphous or crystalline oxides form at the surface of brown Saharan sandstones (figure 1) and give the dark tone of numerous landscapes of this desert. The natural process involves a diffusion of iron, manganese or titanium impurities from the bulk (SiO_2 crystals linked by a cement of $(Ca,K)_2(Al,Fe,Mn,Ti)_3(SiO_4)(Si_2O_7)O(OH)$ clinozoisite) and deposition of complex iron-manganese-titanium oxides at the surface. Adsorption and desorption of water in the pores of the stone are supposed to be responsible of the chemical transport.

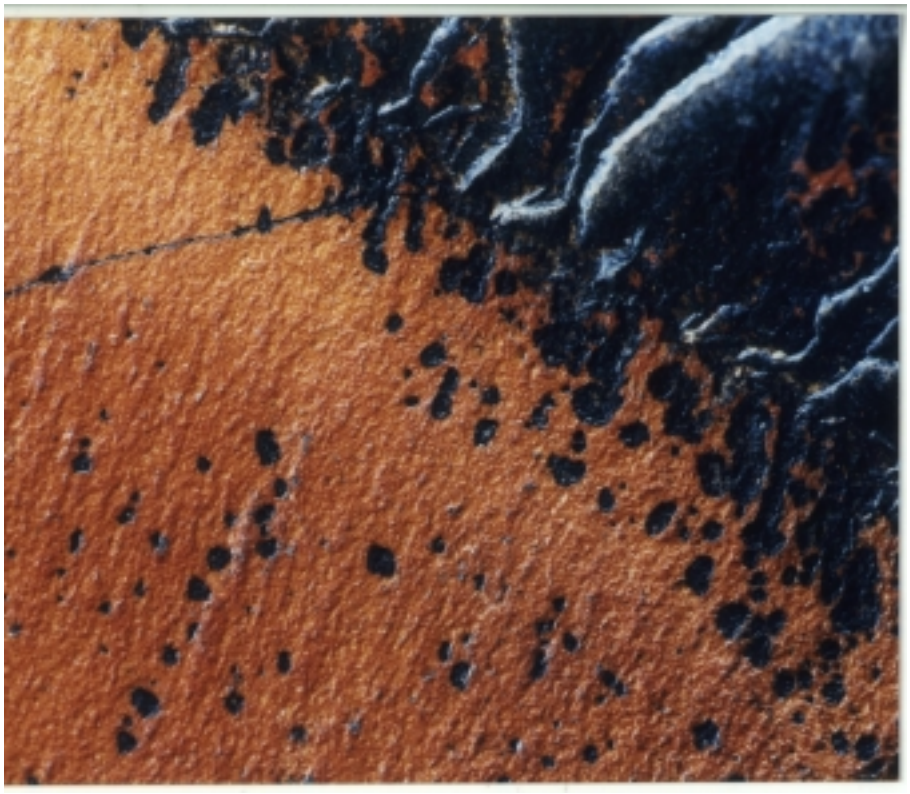

Figure 1. - Crystallisation of iron oxides at the surface of sandstones.

The inverse picture, brown dots on a black surface, can be obtained by coating a stoneware pottery with an iron coloured glaze (oil spot technique). This glaze is generally based on feldspars ($KAlSi_3O_8$ orthose or $NaAlSi_3O_8$ albite), $Mg_3Si_4O_{10}(OH)_2$ talc, $Al_2Si_2O_5(OH)_4$ kaolin, $(Ca,Mg)_2Si_2O_6$ diopside or $CaSiO_3$ wollastonite to which 1-2% Fe_2O_3 are added. Then the potter's art relies on the control of the composition of the materials (natural and/or synthetic), of the temperature cycle and of the atmosphere (reducing or oxidising). The concentration and oxidation states of iron oxides govern the colour (green, iron blues, celadon, iron reds, brown, temmoku) or colour separation (oil spot) and nucleation (wollastonite on sandstone). The firing of stoneware glazes implies decomposition reactions (hydroxides, carbonates), fusion of eutectics, reduction or oxidation, crystallisation and/or vitrification.

Both preceding examples illustrate several "simple" aspects of material elaboration. It is evident that modern science has enormously enlarged the range of usable materials ; consequently, modern technology benefits from very specific and tunable properties of solids, combined with very precise shaping. More and more sophisticated methods of elaboration are used, especially for thin film processing.

The object of this contribution is to give a simple insight into the classical methods of elaboration : the basic principles will be outlined, a brief description of the experiments will be given and examples will be presented and discussed.

A classification of the elaboration methods can be based on :

- the reaction which is involved (solid-solid, solid-liquid, solid-gas)
- the dimensionality of the resulting material (3D = bulk, 2D = thin film)
- the thermodynamic state (stable or metastable phases)
- the crystalline state (single crystal, polycrystalline or amorphous powder, glass ceramic, glass)

Other classification criteria can be found, according to the driving force (temperature gradient, electric or magnetic field), the diffusion or crystallisation mechanisms.

Arbitrarily, we will examine, successively, the following topics : solid state reactions, low and high temperature methods, low and high pressure methods. This choice allows for a simple presentation of the experimental devices.

Generally, high temperature synthesis leads to thermodynamically stable phases, while low temperature favours metastable phases. Low pressure methods are mainly dedicated to thin film coating.

Material elaboration implies matter and energy transfer. This evidence is illustrated by the simple reaction :

$$H_2O_{(liquide)} \rightarrow H_2O_{(solide)} \qquad \Delta H = -\Delta H_m = -L$$

(L = enthalpie de fusion=6.01 kJ.mol^{-1})

Ice crystallisation is exothermic and heat must be evolved from the system. Diffusion of water molecules is involved between the disordered hydrogen bonded liquid and the ordered array of water molecules in the solid state.

The study of water at high pressure has lead to the discovery of several crystalline varieties of ice. They differ only by the relative disposition or orientation (and distances) of water molecules and, consequently, by the hydrogen bonding subnetwork. A representation of the stability domains of ice in the P-T diagram is given in figure 2.

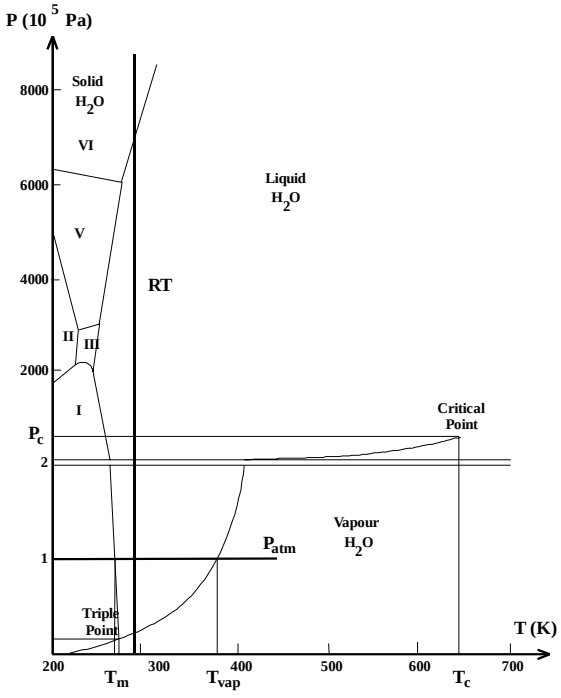

Figure 2. - (P,T) phase diagram of water.

This system illustrates the fundamental questions related to liquid (or gas) phase, solid state and their interaction. What are the microscopic potentials (or structures) which govern the macroscopic behaviour : thermodynamics, dynamics (rotational, translational), physical properties (dielectric constant, thermal expansion, compressibility, density...) ? What is their evolution with the temperature and the pressure, with the presence of foreign species (salts) or at the interface with metals or minerals ? It is shown, for example, that the number of hydrogen bonds per molecule n_{HB}, in liquid water, scales with the density all along the saturation curve. n_{HB} tends to $n_{HB} = 4.0$ at 0°C, like in the solid state, and decreases to $n_{HB} = 1.8$ at the critical point.

The simulation of water is of great practical importance for the characterisation of corrosion phenomena, gas or mineral solubility in hydrothermal fluids (or deep oceanic vents).

The basic thermodynamic functions, which will be used in this chapter, are given in Box 1, together with the corresponding intensive and extensive variables and the associated energy variations. Transport properties and the basic equations of diffusion, or Fick's laws, are given in Box 2. The interpretation of binary (figure 3 and 4.a,b), ternary diagrams (figure 4.c) or (P,T) diagrams (figure 2), is supposed to be known ; in ternary diagrams, at a given composition (P), the ratio between the A, B, C components are given by the ratio of the PA, PB, PC lengths (figure 4.c). However, several simple properties of binary phase diagrams, illustrated in figure 3 are useful for the comprehension of the elaboration techniques.

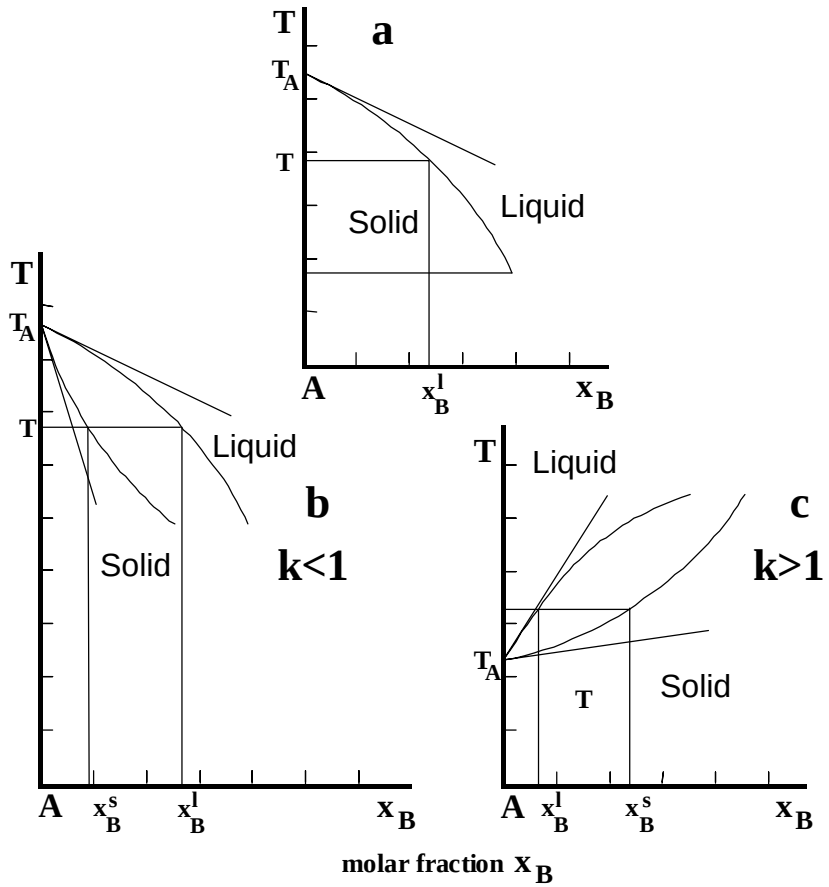

Figure 3. - Parts of A-B binary phase diagrams.

Liquids are supposed ideals and no misciblity (figure 3a) or good solubility (figures 3b and 3c) are supposed in the solid state. A or B compounds are characterised by their molar fraction x_i, their melting temperature T_i associated with the fusion enthalpy ΔH_m^i ; the activity coefficients γ_i are taken to unity. At low concentration, the solubility of B is well approximated by the tangents to the solubility curves.

The following expressions are derived from the equalisation of chemical potentials μ_i of A or B in the solid and liquid phases with :

$$\mu_i = \mu_i^0 + RT \, \mathrm{Log}\, a_i \quad (a_i = \gamma_i x_i)$$

When no misciblity occurs in the solid state (figure 3a), the variation of the crystallisation temperature of A with the addition of a small amount of B is given by :

$$\frac{T_A - T}{x_B^l} = \frac{RT_A^2}{\Delta H_m^A} \qquad \{1\}$$

The solubility of B in the saturated liquid is estimated by : $\mathrm{Log}\, x_B^l = -\frac{\Delta H_m^B}{R}\left(\frac{1}{T}-\frac{1}{T_B}\right)$ {2}

Solutes with high melting points and large enthalpies of melting have low solubility.

In the case of solid state miscibility (figures 3b and 3c), the k ratio (segregation coefficient) between the solubility of small amounts of B in the solid (x_B^s) and in the liquid (x_B^l) is :

$$\mathrm{Log}\, k = \mathrm{Log}\,(x_B^s/x_B^l) = \frac{1}{R}\left[\frac{\Delta H_d^{l,B}}{T} - \frac{\Delta H_d^{s,B}}{T} + \Delta H_m^B\left(\frac{1}{T}-\frac{1}{T_B}\right)\right] \qquad \{3\}$$

with $\Delta H_d^{l,B}$, $\Delta H_d^{s,B}$ = heat of dissolution of molten and solid B into the host lattice and host melt respectively.

The variation of k with the temperature is slow and k is greater or smaller than 1, according to the sign of the expression between brackets in Log k (figures 3b and 3c).

A very simple diagram, LiF-BaF_2, appears in figure 4.a ; it shows:

- a eutectic composition (A),
- a compound formation from the reaction LiF + $BaF_2 \rightarrow BaLiF_3$,
- the peritectic decomposition of $BaLiF_3$ (incongruent melting) to give a liquid B and solid BaF_2.

A phase transition of YF_3 is illustrated in the LiF-YF_3 binary diagram (figure 4.b) ; $LiYF_4$ presents a melting which is close to congruency.

A ternary diagram, given in figure 4c, shows the influence of atmosphere and, particularly, of the oxygen partial pressure : at high temperature, Fe_2O_3 hematite is not stable and its stability range is strongly reduced in a CO_2 atmosphere (thin line in figure 4.c).

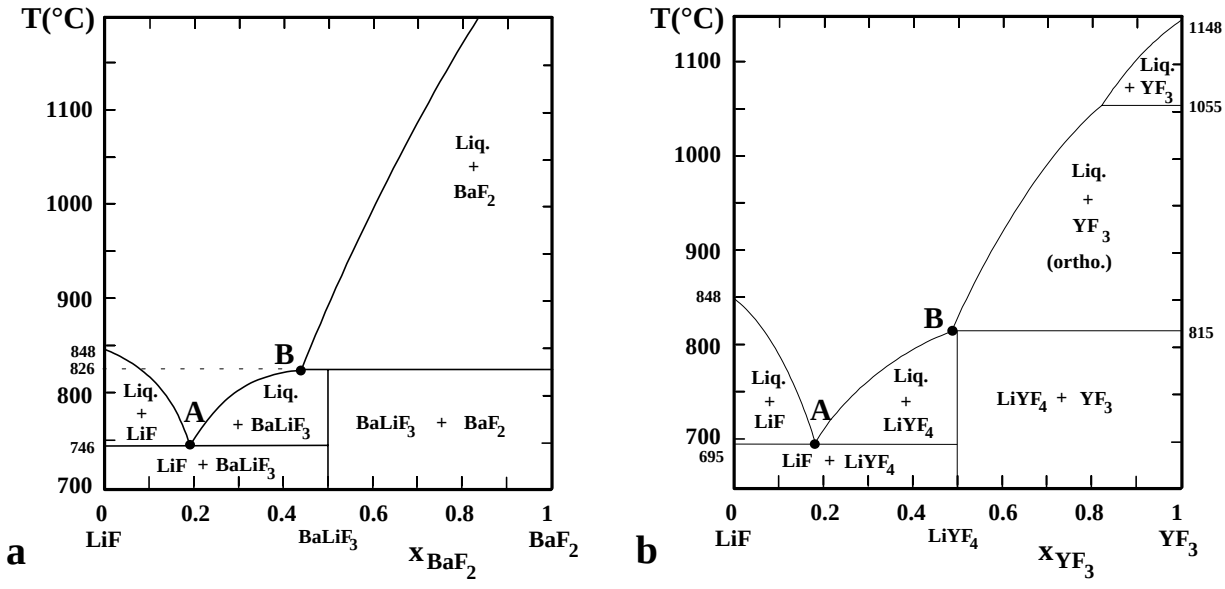

Figure 4. - Binary LiF-BaF_2 (a), LiF-YF_3 (b) phase diagrams.

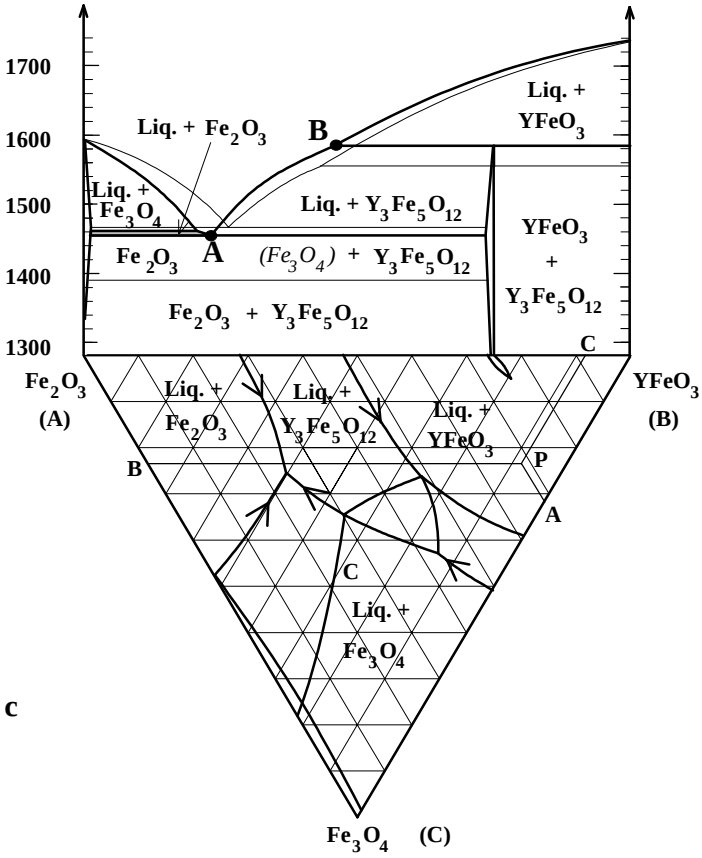

Figure 4(c). - ternary Fe_2O_3-Fe_3O_4-$YFeO_3$ phase diagram.